Characterization of Silk-Elastinlike Proteins For Use in Soft Bodied Robots

An honors thesis
Submitted by

Brian S. Canter

In partial fulfillment of the requirements
For the degree of:

Bachelor of Science
In
Biomedical Engineering

May 2011
Advisor: Professor David Kaplan, Ph. D.
Department of Biomedical Engineering, Tufts University, 4 Colby Street, Medford, MA 02155, USA

Acknowledgements

Thank you to the Tufts University Biomedical Engineering Department for providing guidance and support during this research. I would personally like to thank Xiaoxia Xia and Xiao Hu for being my mentors during the study. They were always there to answer my questions and to provide me with instructions on what to do next. Thank you for helping me carry out all of the experiments. I would also like to thank my advisor Professor Kaplan for allowing me the use of his laboratory and equipment as well as for the idea of the project. I could not have done this study without him.

Table of Contents

Index of Figures

1. Abstract

There are millions of procedures every year that can be classified as invasive or minimally invasive. An additional probe such as a soft bodied robot would be of great use to medical practitioners performing these operations. Such robots are the subject of a project commissioned by the Defense Advanced Research Projects Agency to be used as reconnaissance in urban warfare. However, if these soft bodied robots could be made to both biocompatible and biodegradable then they would be ideal for use in invasive procedures. Silk-elastinlike proteins, which combine the properties of silk and elastin, are one candidate to make this happen. Much of the research concerning these proteins has dealt with their possible use in drug delivery and did not focus as much on production or characterization. This study aimed to optimize the production of silk-elastinlike proteins as well as characterize the material and structural properties of these proteins specifically their transition temperature, secondary structure, and resilience. Two different silk-elastinlike proteins, SE 15 and SE 16, were transformed and expressed in bacterial cells before being purified using column chromatography. CD and FTIR were used to investigate the secondary structure of the silk-elastinlike proteins, while UV-Vis Spectroscopy was used to examine the transition temperature of the materials. AFM was used to determine the resiliency of the silk-elastinlike proteins. Ultimately, SE 16 exhibited transition temperature behavior while SE 15 did not. SE 15 was found to be more resilient than SE 16. These differences are largely due to the disparity in silk units and elastin units between SE 15 and SE 16. The secondary structure of both proteins was found to be composed of mostly unordered structures and beta sheets. While more characterization of these materials is needed before they can be produced to make up soft bodied robots, the results of this study do demonstrate a correlation between the properties of silk-elastinlike proteins and the individual numbers of silk units and elastin units.

2. Introduction

2.1 Clinical Relevance

Each year millions of people incur procedures that can be designated as invasive or minimally invasive procedures. These range from endoscopies that are used to diagnose diseases such as colon cancer to open surgeries such as a triple bypass heart surgery. It would be helpful for a doctor performing a procedure to have an additional probe such as a soft bodied robot at his/her command. In fact such robots are to be used as unmanned reconnaissance on a project commissioned by the Unites States military's Defense Advanced Research Projects Agency. This robot would need to be biocompatible and biodegradable. Past potential robots have been composed of Dragonskin, which is a silicone platinum rubber. These robots cannot be applied to work in the medical field. Thus genetically engineered polymers such as elastinlike proteins and silk-elastinlike proteins have been studied to be used in place of Dragonskin. Elastinlike proteins consist of repeating elastin amino acid peptide sequences that have been grown in an E. coli system using molecular biotechnology (Valieav 2008). Silk-elastinlike proteins exhibit the resiliency of silk with the elasticity of elastin. They are formed by linking silk repeating peptides with the repeating peptides for elastin. These polymers are produced in mass quantities by transforming them into bacteria and using the cell machinery of the bacteria to over express the desired protein. While there has been thorough experimentation involving silk-elastinlike proteins, the mechanical and structural properties of this polymer has yet to be fully examined. Additionally, the optimal conditions for producing large amounts of silk-elastinlike proteins have yet to be precisely determined. Based off previous experiments involving silk-elastinlike proteins, I looked to determine the optimal pH of eluting solutions for the production and purification of silk-elastinlike proteins as well as to characterize the silk-elastinlike proteins as

both protein solutions and protein films. These contributions are significant as they would help researchers better define the material and structural properties of silk-elastinlike proteins providing a platform for them to be used in the future in the composition of a Chembot. In the big picture, this breakthrough in knowledge and research of silk-elastinlike proteins would pave the way for the creation of biocompatible, biodegradable Chembot. These robots could be widely used in humans to detect the onset of disease or to help in performing open surgery. Furthermore, the functions of the Chembot could be tailored to be used in biomedical applications such as a guide in drug delivery or even for repair in tissue engineering.

2.2 Characterization Instruments

2.2a UV-Vis Spectroscopy

UV-Vis spectroscopy is an analytical method that can be used to measure the transition temperature of a protein in solution. This method uses the natural ability of proteins to absorb or scatter light in the UV or visible range (McClements 2011). The wavelength of light used in the ultraviolet range is around 280 nm as this is the wavelength that is best absorbed by tyrosine and tryptophan residues (McClements 2011). In order to determine the transition temperature, the temperature in the UV-Vis spectrometer needs to be increased. As this temperature is increased, a protein in solution will undergo a transition from a solution state to a turbid state (Nagarsekar 2002). The transition temperature is then defined as the temperature at which the protein reaches half of its maximum absorption value (Nagarsekar 2002).

2.2b Circular Dichroism

Circular dichroism (CD) is a method that is widely used to examine the secondary structure of proteins. CD is described as the unequal absorption of left and right circularly polarized light (Greenfield 2006). Light is characterized by having time dependent electric and

magnetic fields associated with it, and if it becomes polarized by being passed through a filter, its electric field will oscillate. (Greenfield 2006). This field will oscillate sinusoidally, and the resulting wave can be seen as a combination of two vectors of equal length with one rotating clockwise or right, and one rotating counterclockwise or left (Greenfield 2006). Asymmetric molecules may then interact with the light such that they absorb more or less right or left circularly polarized light (Greenfield 2006). This results in the plane of the light wave being rotated and the two vectors tracing out an ellipse making the light elliptically polarized (Greenfield 2006). CD is usually reported in degrees ellipticity referring to the angle, which has a tangent that is equivalent to the ratio of the minor to major axis of the ellipse (Greenfield 2006). The secondary structure of proteins can be determined using CD as when the chromophores of the amides of the polypeptide backbone of proteins line up, exciton interaction cause their optical transitions to shift or split into multiple transitions (Greenfield 2006). Therefore, different secondary structure elements such as beta sheet and alpha helices will have characteristic CD spectra (Greenfield 2006).

2.2c Fourier Transform Infrared Spectroscopy

Fourier Transform Infrared Spectroscopy (FTIR) is another widely used method to estimate the secondary structure of proteins. FTIR is a preferred method of infrared spectroscopy, where infrared radiation is passed through a sample and is either absorbed or transmitted ("Molecular Materials Research Center" 2001). In FTIR, an interferometer is employed, which encodes all frequencies of infrared light into one signal ("Molecular Materials Research Center" 2001). This allows for the spectrum of all frequencies of infrared light to be calculated at once. Fourier transformation is used to decode the signals from the interferogram into a frequency spectrum that can be easily interpreted ("Molecular Materials Research Center

2001"). Every sample has a specific characteristic set of absorption bands in its infrared spectrum (Gallagher 2005). For proteins the Amide 1 and Amide 2 are two characteristic bands that form their infrared spectra (Gallagher 2005). They are due to the presence of amide bonds that connect amino acids through hydrogen bonding (Gallagher 2005). The stretching vibrations of the C=O bond are correlated with absorption of the Amide 1 bond, while absorption of the Amide 2 bond affects bending vibrations of the N-H bond (Gallagher 2005). Since both of these bonds are involved in the hydrogen bonding that occurs between different secondary structure elements, the Amie 1 and Amide 2 bands are dependent on the secondary structure for that specific protein (Gallagher 2005).

2.2d Atomic Force Microscopy

Atomic Force Microscopy (AFM) is an instrument that can be used for sensitive force measurements as well as high resolution imaging of microscopic particles (Owen 2010). The tip of the AFM instrument is sensitive to small forces and is suspended on the AFM cantilever, which is a soft spring (Owen 2010). For imaging of samples, the cantilever is run over the surface producing a three dimensional image (Owen 2010). For force spectroscopy experiments, the cantilever and tip approach the surface of the sample, make contact with it, and are then retracted all while the interactions between tip and sample are measured (Owen 2010). AFM can be used for proteins to investigate a variety of material properties. Specifically, as the tip makes contact with the protein sample, it can be used to measure the stiffness and viscoelastic response of the protein (Owen 2010). Additionally, the output of the AFM force spectroscopy experiments is a force curve diagram that depicts the deflection of the cantilever versus the height of the cantilever and tip as they approach and retract from the sample (Owen 2010). These force curves can then be analyzed to determine material characteristics and properties for the protein.

3. Background

3.1 Elastin

Elastin is a natural polymer found in the arterial cell walls of Mammalian animals (Valieav 2008). The polymer itself is insoluble, hydrophobic, and extensively crosslinked with other proteins (Debelle 1999). It contributes to the ability of arteries to constrict and expand allowing for blood flow (Valieav 2008). Also, it is responsible for the resilience of tissues found in the skin, arteries, and lungs (Debelle 1999). The function of elastin is limited to elasticity but this property is not fully understood (Debelle 1999). There are three models that attempt to account for the elasticity of elastin. The first model characterizes elastin as a random chain polymer, with entropic elasticity (Valieav 2008). This model helps to explain the high mobility of the elastin backbone (Valieav 2008). However, it fails to address the solvent polypeptide interactions, which play a crucial role as elastin only displays elasticity in the presence of solvents (Valieav 2008). The second model focuses on using the librational entropy of peptide segments moving between the secondary structures of beta sheets (Valieav 2008). Finally, a third model to account for this property of elastin characterizes the polypeptide as globular protein regions in aqueous diluents (Valieav 2008).

3.1a Precursor and Structure

There have been studies done reviewing the structure of elastin. The precursor to elastin is tropoelastin, which has found to contain similar sequences, despite the presence of alternative splicing, in a variety of organisms (Debelle 1999). The secondary structure of tropoelastins is mostly composed of beta sheets and unordered structures and was studied using FTIR and CD (Debelle 1999). Elastin is composed of crosslinked tropoelastin molecules, and its secondary

structure was found to be composed mostly of beta sheets and unordered structures (Debelle 1999). This was done using NIR FTR and FTIR spectroscopies (Debelle 1999). Overall, this confirms that the structure of tropoelastin and elastin are similar (Debelle 1999). In fact a tridimensional proposed model of elastin suggests that elastin is composed of globular, regularly aligned tropoelastin molecules crosslinked with adjacent molecules (Debelle 1999). The addition of water to elastin causes it to swell (Debelle 1999). Additionally, the presence of water disrupt the structure of the polypeptide especially if it is in the form of a bulk solvent (Debelle 1999).

3.1b Use in Crosslinking

Researchers have also looked into synthesizing recombinant elastin mimetic proteins capable of physical and chemical crosslinking (Sallach 2009). They first constructed the synthetic genes of both the elastin and chemical crosslinking domains using genetic engineering. Next, they assembled the elastin polymers before they isolated and purified them. After that, they ran a rheological analysis of the proteins before casting them into films for mechanical property analysis. Lastly, they evaluated the crosslinked protein gel in vivo using histological examinations as well as fluorescent activated cell sorting. The experimenters determined that they were able to produce viscoelastic protein gels (Sallach 2009). Furthermore, they observed that crosslinking increased the elastic modulus and strength of the polymers, it decreased the resilience (Sallach 2009). Lastly, they found that implanted elastin mimic proteins did not produce any significant inflammatory or allergic reactions (Sallach 2009).

3.1c Use as a Connective Tissue

Since elastin is a main component of connective tissue, there has been work done to examine whether elastin can be incorporated with polyethylene terephthalate to form viable, biofunctional matrices for use as vascular prostheses (Dutoya 2000). They first prepared elastin solubilized peptides (ESP) that were incorporated with polyethylene terephthalate (PET) (Dutoya 2006). Then they used scanning electron microscopy as well as transmission electron microscopy to perform microstructural analysis of the composite compound (Dutoya 2006). Furthermore, they ran biologically assays to assess the attachment, proliferation, morphology and characterization of endothelial cells on the material composed of ESP-PET (Dutoya 2006). The results of microstructural analysis experiments demonstrate that at a microscopic level, ESP coatings are covering the PET fibers (Dutoya 2006). Biological analysis of the endothelial cells being grown on the composite material showed no effects of cytotoxicity (Dutoya 2006). Also, the ESP coating decreased cell attachment to ESP-PET (Dutoya). The coating of ESP onto PET resulted in decreased cell proliferation as well (Dutoya 2006). Ultimately, more work is necessary in order to determine the effects of using elastin in a matrix that will function as vascular prostheses, but this study served as a solid initial step in the process.

3.2 Silk

Silk is another natural polymer that is derived from spiders and silkworms (Altman 2003). It has been used for years in textiles as well as medically for sutures (Altman 2003). It contains a general repeating amino acid sequence similar to: Gly–Ala–Gly–Ala–Gly–Ser (Altman 2003). Silk is generally composed of beta sheet structures as short side chain amino acids that are hydrophobic dominate interactions (Vepari 2007). These proteins are both remarkably strong and tough (Altman 2003). They also are much more resistant to failure than other materials exhibiting similar strength and toughness (Altman 2003). In addition, the

immune response to silk that has been seen from its use in sutures is not directly a result of the silk material but rather of the geometry and shape of the suture (Altman 2003). Lastly, silk is biodegradable over the long time as in it can and will be broken down by the body (Altman 2003).

3.2a Artificial Construction and Expression

It has been shown that synthetic spider silk genes can be artificially cloned, constructed, and expression using genetic engineering (Prince 1994). The researchers began with the construction of the pUC-LINK plasmid was accomplished by adding a synthetic adapter into the pUC18 vector. Then the synthetic spider silk DNA fragments were constructed, and afterwards the synthetic silk multimers were constructed using two different approaches. They were then transformed into bacteria and identified using enzymes with restriction analysis. Protein expression was then enhanced with the addition of IPTG, and expression levels were verified using SDS-PAGE. The cells were lysed by centrifugation, and Ni-NTA column chromatography was used to purify the protein and further purification was carried out using reverse phase HPLC. Additionally, the proteins were characterized using HPLC and circular dichroism. The SDS-PAGE gels displayed that the synthetic silk protein had been produced while HPLC and circular dichroism results also confirmed this result (Prince 1994). Ultimately, the scientists were able to demonstrate that it was possible to artificially construct and express silk proteins.

3.2b Use in Biomedical Applications

Currently silk is being used in a variety of applications in biomedical engineering. This material can be formulated into gels, sponges, or films (Vepari 2007). In addition, its amino acid side chains can be changed to allow for a change in surface properties or immobilize cellular growth factors (Vepari 2007). Silk can be used in cell recognition or mineralization through

modifying it with molecular engineering (Vepari 2007). Different cell lines have been successfully grown on silk to illustrate a variety of biological outcomes (Vepari 2007). Finally, silk scaffolds have been employed to grow bone, cartilage, tendon and ligament tissues (Vepari 2007).

3.3 Elastinlike proteins

Elastinlike polypeptides are composed of the repeating pentapeptide sequence Val-Pro-Gly-X-Gly, where x is any amino acid except proline (Valiaev 2008). They are stimuli responsive and are produced using genetic engineering (Valiaev 2008). A synthetic plasmid containing the gene for production of the repeating pentapeptide sequence is overexpressed in E. coli. Elastinlike proteins have been shown to be easily manufactured and their composition and chain length can be easily controlled (Valiaev 2008). They can be manipulated for force generation and are suitable building blocks for engineered protein elastomers (Valiaev 2008).

3.3a Lower Critical Solution Temperature

One important property of elastinlike proteins is their lower critical solution temperature (LCST). The LCST of elastinlike proteins is the temperature at which the polypeptides no longer are soluble in water and form a large aggregate (Valiaev 2008). This is a rapid phase transition that causes the protein to aggregate and come out of solution (Valiaev 2008). This property can easily be influenced based on the primary structure depending on which amino acid is used as some amino acids are more hydrophobic than others (Valiaev 2008). Therefore unlike other polymers that exhibit this property, it is easier to tune the LCST to the desired temperature of interest (Valiaev 2008).

In addition, it has been shown that the secondary structure of elastinlike proteins can have an effect on the lower critical solution temperature (LCST) of these proteins has been examined

(Nuhn 2008). Specifically, the chain length and chemical composition of the polypeptides that comprise these proteins were studied in short elastinlike polypeptides which are composed of only 1-6 pentapeptide repeats (Nuhn 2008). The researchers used Fmoc solid phase peptide synthesis to create the short elastinlike polypeptides. These polypeptides were varied in length to study the effect of chain length on secondary structure formation. In order to study the effect of amino acid structure, valines found in the repeating pentapeptide where replaced with isoleucine, leucine, and phenylalanine all of which are more hydrophobic (Nuhn 2008). The group calculated the partition coefficient, which is the molar equilibrium concentration ratio of a given species between two phases usually water and octanol, and used it as an estimate of the hydrophobicity of the short elastinlike polypeptides (Nuhn 2008). The partition coefficients were then used to calculate the expected LCST as there is a direct relationship between hydrophobicity and this property (Nuhn 2008). They then used circular dichroism to investigate the change in secondary structure of the protein with respect to temperature, and they used UV-Vis spectroscopy to determine the lower critical solution temperature in the polypeptides. The lower critical solution temperature was found to increase when the polymer chain was shortened (Nuhn 2008). Additionally, changing the amino acid structure, specifically replacing valines with more hydrophobic amino acids, resulted in a change in the secondary beta structures of the polypeptides (Nuhn 2008). This resulted in a decrease in the lower critical solution temperature. While these results as stated in the study do suggest useful biomaterials that could be implemented in biomedicine and engineering, there is not a thorough explanation of how the secondary structure changed on the proteins. All that was noted was the secondary beta structure became more ordered and distinct at higher temperatures.

3.3b Elasticity

Furthermore, work has been done on analyzing the elasticity of elastin like proteins and how they are impacted by changes in temperature, ion strength, solvent polarity, and guest residues (Valiaev 2008). This was done by examining elastinlike proteins chemically grafted onto self assembled monolayers to display a distinct hydrophilic-hydrophobic transition. The researchers used Atomic Force Microscopy specifically Single Molecular Force Spectroscopy to obtain force extension curves for the treated elastinlike proteins (Valiaev 2008). Furthermore, they used the freely jointed chain model to provide analysis for the force extension behavior of the elastinlike proteins and directly did this by measuring the Kuhn segment length (Valiaev 2008). At an individual elastinlike protein level, the length of the Kuhn segment could be used to approximate the elasticity of the elastinlike protein (Valiaev 2008). The results of the experiment showed that there was an optimal temperature range, where elasticity of the proteins peaked (Valiaev 2008). In addition, the results of the experiment demonstrated that increasing the temperature in elastinlike proteins directly affects the energetic changes in stretching an elastinlike protein molecule (Valiaev 2008). Also, an increase in ion strength increased the elasticity of the protein as did an increase in solvent polarity (Valieav 2008). This means that in solutions with higher ion concentrations it is easier to stretch the elastinlike proteins. Lastly, the most hydrophilic polymer with therefore the most hydrophilic guest residue was shown to have the highest elasticity (Valiaev 2008). This study was groundbreaking in the sense that it was one of the first to examine the effect of solvent on elastinlike proteins.

3.3c Use in Crosslinking

The feasibility of crosslinking elastinlike proteins has also been explored (Lee 2009). In this experiment elastinlike proteins were crosslinked using dicumyl peroxide and the

crosslinking was compared to two proteins that were crosslinked using gamma radiation (Lee 2009). The equilibrium swelling ratio of the fibers comprising the crosslinked proteins was measured by immersion in DMSO and water in order to determine the optimization of the crosslinking reaction (Lee 2009). Also, this ratio was measured with respect to a change in temperature. Additionally, ATR-FTIR analysis was performed to determine whether the crosslinking caused any side reactions to occur. The scientists used uniaxial tensile tests to investigate the Young's modulus for each of the crosslinked polypeptides (Lee 2009). Lastly, they used laser scanning confocal fluorescence microscopy to visualize the structures of proteins crosslinked at two different temperatures, one below the transition temperature and one above the transition temperature. The researchers found that the reaction temperature and time range had an effect on the cross linking temperature for the elastin like proteins (Lee 2009). They concluded that there was an optimal range in each measurement for the process to occur (Lee 2009). They also found that manipulating the DCP content could control the crosslinking density of the protein (Lee 2009). The ATR-FTIR results demonstrated that there was no difference in the chemical nature of the proteins that were crosslinked (Lee 2009). The laser scanning confocal microscopy results displayed that elastinlike proteins crosslinked above the transition temperature have a distinct structure (Lee 2009). Furthermore, the results of the uniaxial tensile test were used to assess the crosslinking density which did not seem to be affected by a change in temperature of the crosslinking reaction (Lee 2009). While this was a thorough investigation of the crosslinking of elastinlike proteins, the process of crosslinking elastin like proteins was not connected to any possible real world applications.

There have been studies dedicated to the use of crosslinked elastin proteins in tissue engineering. In particular, the use of these proteins was studied for bladder reconstruction (Urry

1997). Bioelastic matrices were synthesized with elastin protein based materials that were designed for urothelial cell growth such that the elastic modulus of the matrices would resemble that of natural tissue. Then normal human ureter explants were placed on this matrix. The morphology of the cells was tracked using expression of cytokeratin-8. The preliminary results of the experiments found that urothelial cell outgrowth expanded and became denser when grown on an elastin like protein (Urry 1997). These preliminary results are promising but further in depth testing would need to be done to truly see if elastin proteins can be used as biomaterials.

3.4 Silk-Elastinlike Polypeptides

Silk-elastinlike proteins are composed of both elastin and silk units. They are constructed by combining the repeating sequence blocks found in elastin and silk to create a new genetically engineered material that is the silk-elastinlike protein (Ner 2009). This material exhibits a combination of the material properties of both elastin and silk (Ner 2009). This means that it has the elasticity of elastin and the strength and toughness of silk making it a unique material, which would be impossible to create through means other than molecular engineering. It is possible to express the silk-elastinlike protein gene in a non native organism such as E. coli by introducing it through transformation (Ner 2009). Here, the repeating silk and elastin sequences would be placed in plasmid that would then be introduced to culture cells. The protein expression could then be optimized in the cells and eventually extracted from the bacteria.

3.4a Synthesis and Transition Temperature

There been work done on examining polymers that are silk-elastinlike proteins and how they respond to changes in the surrounding environment (Nagarsekar 2002). Researchers synthesized silk-elastinlike proteins and then described their characterization with regards to pH,

temperature, ionic strength, and concentration (Nagarsekar 2002). Specifically, silk-elastinlike constructs were ligated into an acceptance plasmid and then made in E.coli bacteria cells. After being selected, they were ligated into a different expression vector and retransformed into E.coli for protein expression. The transition temperature of the silk-elastinlike proteins was measured using turbidity studies with spectrophotometer. Ultimately, the transition temperature (Tt), which is the same as the lowest critical solution temperature was found to increase when the pH was increased (Nagarsekar 2002). Also, an increase ionic strength caused the transition temperature to decrease (Nagarsekar 2002). The addition of more polymer or an increase in concentration caused the transition temperature to decrease as well (Nagarsekar 2002). These results do demonstrate the potential of using silk-elastinlike proteins as their transition temperature can be modified and manipulated by changing an external factor in the solution such as pH or ion concentration. They can be easily genetically engineered to be used in a sundry of biomedical applications.

3.4b Use in Drug Delivery

One biomedical application that has been thoroughly explored for the use of silk-elastinlike proteins is drug delivery. There has been a lot of experimental work done to investigate the properties and characteristics of silk-elastinlike proteins as hydrogels for possible use in drug delivery. In one experiment, researchers examined solute diffusion in silk-elastinlike protein hydrogels (Dinerman 2002). They specifically looked into the effect of the polymer volume fraction and the gelation time on diffusivity and partitioning of the hydrophilic molecules theophylline, Vitamin B12 as they were in the size range of most therapeutic proteins and molecules (Dinerman 2002). A model protein cytochrome c was also used to assess the impact of the hydrogel loading method as well as the gelation kinetics. After hydrogel

preparation, the researchers subjected them both to equilibrium swelling tests involving all three hydrophilic molecules as well as diffusion studies involving just the model protein cytochrome c. It was found that diffusion behavior in silk-elastinlike protein hydrogels is size dependent (Dinerman 2002). Also, it was seen that size exclusion by itself cannot account for the observed partition coefficients meaning there must be other interaction responsible in silk-elastinlike protein hydrogels (Dinerman 2002). Furthermore, directly incorporating a protein in the silk-elastinlike protein hydrogel solution did not have an effect on its release profile (Dinerman 2002). The results of this experiment do characterize the behavior of silk-elastinlike protein hydrogels and exhibit their potential use as deliverers of therapeutics.

Researchers have also looked into electrospinning silk-elastinlike proteins for use in drug delivery (Ner 2009). The scientists electrospun the silk-elastinlike proteins in water and looked to determine the effect of this process on fiber morphology and fiber diameter. They used a polarized light microscope as well as a scanning electron microscope to image the electrospun fibers of the protein. Lastly, they also used FTIR and X-Ray diffraction to examine the secondary structure of the electrospun protein fibers. The results of their experiment detailed the fiber morphology and characteristics and detailed the effect of several electrospinning parameters on the protein fibers (Ner 2009). They were able to use the output from FTIR to indicate the presence of secondary structures in the protein including random coils and beta sheets (Ner 2009). These same results were then able to be confirmed by X-Ray diffraction (Ner 2009). Ultimately, this experimental work made a large contribution as it strengthened the belief that silk-elastinlike proteins in the form of electrospun fibers could be manipulated to be used in drug delivery.

There have also been experiments done that biologically evaluated the silk-elastinlike polymers as well as assessed their ability to deliver DNA as a therapeutic (Megeed 2002). The resorption of silk-elastinlike films was evaluated by implanting them into lab rats for seven weeks. The result of this experiment was that the resorption of silk-elastinlike proteins is controlled by the length of the silk units and not by the elastin to silk ratio (Megeed 2002). This displays the concept that the structure of silk-elastinlike proteins can be tailored to fit a desired degradation profile (Megeed 2002). In addition, the biocompatibility of the silk-elastinlike films was measured by viewing the histology of the implanted films over the course of the implantation. The results revealed only a mild immune response, which was confirmed using sponges composed of silk-elastinlike proteins (Megeed 2002). In this experiment there was found to be no evidence of chronic inflammation (Megeed 2002). Further testing in pigs involving the response in wound tissue to silk-elastinlike proteins as well as immunogenicity testing in rabbits demonstrated the biocompatibility of silk-elastinlike proteins (Megeed 2002).

3.4c Formulation into Hydrogels

Another group of researchers also have examined the behavior of silk-elastinlike proteins as hydrogels (Dandu 2008). They investigated the influence of structural changes on equilibrium swelling under a variety of external conditions, mechanical properties and pore structure of the hydrogels using a number of characterization instruments (Dandu 2008). First, the researchers constructed their own silk-elastinlike proteins using genetic engineering and then formulated them into hydrogels. They then performed equilibrium swelling studies as well as dynamic mechanical analysis and small angle neutron scattering. They observed that silk-elastinlike proteins with lower ratios of silk units to elastin units required more polymer chains to assemble in hydrogels (Dandu 2008). Additionally, the equilibrium studies revealed that polymer structure

and concentration are the major facts impacting the degree of crosslinking in silk-elastinlike protein hydrogels (Dandu 2008). The cure time of the hydrogel as well as the ionic concentration of the solvent also influence the crosslinking while the pH and temperature of the solution do not seem factor in (Dandu 2008). The mechanical testing and structural testing affirmed the assertion that the silk units offer strength and rigidness to the hydrogel while the length of the elastin units affects the spacing of the crosslinking (Dandu 2008).

Additionally, in order to deliver DNA as a therapeutic, the challenges of the high size and charge of DNA must be overcome while controlling the rate and location of the release and protecting against nuclease degradation (Megeed 2002). The release of plasmid DNA from silk-elastinlike protein hydrogels has been examined and was modeled in an equation that described two dimensional diffusion from a cylinder (Megeed 2002). The data show that the release profile resembles that of Fickian diffusion (Megeed 2002). The release rate was affected by the polymer concentration and cure time but not by the DNA concentration (Megeed 2002). All in all, the silk-elastinlike protein hydrogel showed a lot of promise for an effective and targeted delivery of DNA.

Researchers have further expanded testing on silk-elastinlike protein hydrogels to include the release of adenoviruses using these proteins (Gustafson 2010). The idea behind these studies is that silk-elastinlike protein hydrogels could be used to carry therapeutics for the treatment of cancer in patients if they can control delivery and distribution (Gustafson 2010). The scientists tracked the release of the adenovirus using green fluorescent protein. The results of this study were not quantitative but they did indicate that the concentration of the silk-elastinlike protein influenced the release of the adenoviruses (Gustafson 2010). Those hydrogels with less concentrated protein were able to release drugs for a substantially longer amount of time

(Gustafson 2010). Another study using silk-elastinlike proteins in a similar manner quantified the release of the virus using RT-PCR. The results of this experiment suggested that a silk-elastinlike protein hydrogel could control the time and place of the virus transfection but that around 30-40 percent of the virus was lost while being incubated with the protein (Gustafson 2010). Overall, silk-elastinlike proteins do show potential to be used in the future as a delivery method for the treatment of cancers.

3.4d Characterization of Similar Protein

Silk-tropoelastin proteins contain repeating units of the elastin precursor tropoelastin. It is an optimal biomaterial as it displays elastomeric behavior and is naturally found in human tissue (Hu 2010). In a recent study researchers synthesized several blends of silk-tropoelastin proteins to observe the interaction of the two proteins with respect to material properties as well as with cells (Hu 2010). The blends were synthesized not using a cell culture system. The phase transition temperature of the silk-tropoelastin blends was investigated using differential scanning calorimetry. The secondary structure of the proteins was analyzed using FTIR. AFM was used to determine the elasticity of the proteins. Lastly, the researchers seeded human mesenchymal stem cells onto the silk-tropoelastin blends and tracked their proliferation using an MTT assay. The results of the experiment demonstrated the different mechanical properties, structure, and cell interactions depending on the specific blend of silk-tropoelastin (Hu 2010). Overall, the experimenters were able to demonstrate that the properties of silk and tropoelastin were conserved when blended together and that they interacted favorably with human stem cells (Hu 2010). The simplicity of the blending these silk-tropoelastin proteins makes this strategy a solid choice for future work involving the proteins.

4. Experimental Work

4.1 Objectives

While silk-elastinlike proteins have been well researched, the majority of this is for use in drug delivery. There has been only a little amount of research that has focused on determining the optimal production conditions for these proteins. Therefore, the first objective of this study is to investigate the optimal conditions for silk-elastinlike protein production and to fill in this gap in the literature. This is significant as production conditions would need to be determined for silk-elastinlike proteins if they were to be used in Chembots. Additionally, outside of the transition temperature property, the material and structural properties of silk-elastinlike proteins are not well documented. Therefore, the second objective of this study is to determine the structural and material properties of silk-elastinlike proteins. This is significant as it is necessary to know the material and structural properties of these proteins if they are going to be used as a polymer material in a Chembot. This is the case as the Chembot will need to have the ability to constrict to a certain size and then reexpand to its original volume. It will also need specific proteins for specific parts such as the sensors and actuators.

4.2 Specific Aims and Hypothesis

Aim 1: Assess the effect that the pH of a solvent solution has on the production of silk-elastinlike proteins. My hypothesis indicates that I believe that optimizing the production of silk elastinlike proteins will determine the pH of the solvent solution that produces the maximum yield. The expected outcome for each silk-elastinlike protein will be a protein solution with a pH of 4.5, which is the pH for the elution buffer used in purification.

Aim 2: Identify the effect that the amino acid primary structure has on the material and structural properties of silk-elastinlike proteins. My working hypothesis focuses on the effect

that the amino acid primary structure, which is directly related to the number of elastin and silk residues that make up the silk-elastinlike protein, will have on the transition temperature, secondary structure, and resilience of the silk-elastinlike proteins. Resilience is being defined as the maximum elastic energy that can be absorbed by the protein. The expected outcome for this aim will be calculated transition temperature values, calculated amounts of secondary structure elements, and calculated resilience values for each protein.

4.3 Approach

Figure 1. A flowchart depicting the approach for this study.

4.4 Materials and Methods

4.4a Glycerol Stock Preparation

Two microliters of plasmid pET30a containing the DNA of SE 15 or SE 16 (Figures 2 and 3) was added to fifty microliters of BL-21 chemically competent cells (Invitrogen). The cells were heat shocked for thirty seconds at forty two degrees Celsius before being put on ice for two minutes. They were then added to 400 microliters of SOC medium and placed in the thirty seven degree shaker for forty minutes. Then they were each plated onto two LB agar plates containing kanamycin (twenty five micrograms/milliliter) and left at thirty seven degrees overnight. Cultures were plated at densities of one to one and one to ten. One colony from each of the SE 15 and SE 16 plates were selected and inoculated overnight with five milliliters of LB medium and five microliters of kanamycin at thirty seven degrees Celsius. Next, ten microliters

of these cultures were inoculated with five milliliters of LB and five microliters of kanamycin and placed at thirty seven degrees Celsius overnight. Then fifty microliters of the previously inoculated cultures were inoculated with five milliliters of LB and five microliters of Kanamycin. They were then placed in the thirty seven degree shaker overnight. Glycerol stocks were then made by adding two hundred microliters of these cultures to two hundred microliters of glycerol.

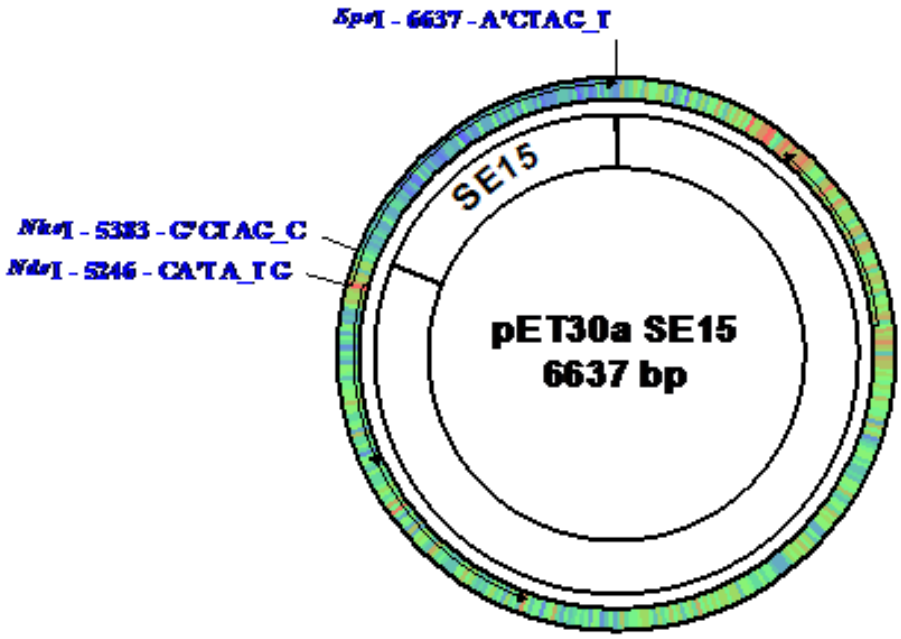

Figure 2. A pET30a plasmid containing the gene for SE 15 as well as restriction enzyme sites for SpeI, NheI, and NdeI.

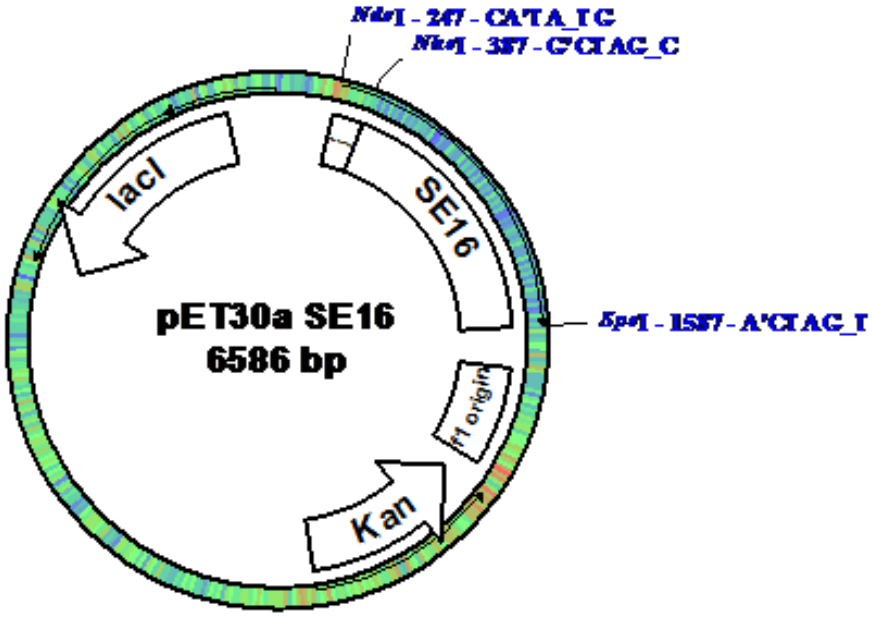

Figure 3. A pET30a plasmid containing the gene for SE16 as well as a selective resistance for kanamycin, a gene for the lacI operon, and an f1 origin. There are also restriction enzyme sites for SpeI, NheI, and NdeI.

4.4b Small Scale Expression

Twenty microliters of the glycerol stocks of SE15 and SE16 were inoculated in five milliliters of LB and five microliters of kanamycin and left to grow overnight. 200 microliters of each of the cultures were then combined with twenty milliliters of LB and twenty microliters of kanamycin and were shaken at thirty seven degrees Celsius for 150 minutes. The OD was then measured for 400 microliters of both cultures. The cultures were then induced to express SE 15 and SE 16 proteins respectively with the addition of twenty microliters of IPTG. The optical density was measured again for both cultures two hours after induction and four hours after induction. Culture samples to be used for SDS-PAGE after zero, two, and four hours of induction with IPTG were equilibrated to have the same amount of cells using their optical densities. These samples were then dissolved in ten microliters of phosphate buffered saline and

added to 3.33 microliters of 4XLDS Buffer (Invitrogen). They were then heated for ten minutes and were loaded onto the NuPAGE Novex 4-12% Bis-Tris gel, which was placed in five percent MES running buffer. A Novex Sharp standard ladder (Invitrogen) was also loaded onto the gel. The gel was run for forty five minutes at 200 volts, 500 milliamps, and 150 watts. After that, the gel was placed in a fixing solution (twenty milliliters water, five milliliters acetic acid, twenty five milliliters methanol) on a horizontally shaking plate. Then the fixing solution was discarded and it was placed in a staining solution, which was part of a Colloidal Blue staining kit [27.5 milliliters water, ten milliliters methanol, ten milliliters stainer A (Invitrogen)] for ten minutes on the same plate. Lastly, the staining solution was removed and 2.5 milliliters of stainer B (Invitrogen) was added to the gel and left overnight on the plate. The gel was then destained using deionized water and imaged using a gel box Computer program (Syngene).

4.4c Large Scale Expression

First start cultures were prepared using 100 microliters of glycerol stock and two milliliters of LB with two milliliters of kanamycin. The cultures were shaken for eight hours at thirty seven degrees and then were placed overnight in the refrigerator. 100 microliters of these cultures were inoculated with 500 milliliters of LB and 500 microliters of kanamycin and were left shaking at thirty seven degrees overnight. They were then induced with 500 microliters of IPTG and left to grown for five hours. After that, the cell cultures were spun down for twenty minutes at 4000 rpm. The supernatant was discarded and a denaturing buffer Buffer B (13.8 g sodium hydrogen phosphate, 1.2 g Tris Base, 480.5 g Urea per liter), which has a pH of 8.0, was added to the cell culture pellet. These mixtures were left spinning overnight and were then spun down at 8700 RPM. The solutions were decanted and the supernatant was collect. 1 milliliter of

Ni-NTA beads were then added for every four milliliters of supernatant the supernatants were placed in the refrigerator.

4.4d Large Scale Purification

Both the SE 15 and SE 16 samples were then loaded into purification columns. The supernatant was then allowed to flow through the column, leaving only the beads in the column, and was collected in thirty milliliter conical tubes (Falcon). Fifteen milliliters of Buffer B were then run through the columns and the flow through was collect as well. This process was then repeated with thirty milliliters for Buffers C, D, and E. All of these buffers have the same chemical composition as Buffer B but have different pH values of 6.3, 5.9, and 4.5 respectively. Two different samples were collected for Buffer E as it was run through the beads in two increments of fifteen milliliters. These were designated E1 and E2. 4.5 microliters of the purified Buffer B, C, D, E1, and E2 samples were then each combined with 2.5 microliters of 4XLDS sample buffer, 2 microliters of water, and one microliters of a 10X reducing agent (Invitrogen) and loaded in the same way onto an SDS-PAGE identical to the one used in small scale expression. The gel was then run and treated with the same fixing and staining solutions as in small scale expression. It was then destained and a picture was taken using the same computer, gel box, and software as small scale expression.

4.4e Repurification

Large scale purification was then carried out in the same manner as described above except the pH of each of the buffer solutions was first verified using an electronic pH meter (Mettler Toledo).

4.4f Dialysis and Determining Concentration of Protein

The supernatant corresponding to E1 and E2 for SE 16 was then loaded into a Slide Analyzer Dialysis Cassette (Thermoscientific) and placed in two liters of water. It was then spun on a stirring plate constantly for one week. The water was changed at least once a day, and at the end of the dialysis, the purified protein was placed at four degrees Celsius. The concentration of this SE 16 protein along with an SE 15 lab stock protein were measured used a bicinchoninic acid protein assay (BCA). First, the seven standard solutions from the BCA kit were prepared from stocks provided in the manufactured kit and water (Invitrogen). Then the working reagent was made using ten microliters of reagent A and 200 microliters of reagent B. After, twenty five microliters of each standard solutions was placed in the first two columns of a ninety six well plate. Then twenty five microliters of the unknown samples were added to into the well. Lastly, the working reagent was added in 200 microliter aliquots to each of the wells. The well plate was then incubated at thirty seven degrees for thirty minutes and the absorbance of each sample in the well was calculated. The absorbencies of the standard solutions with known concentrations were used to plot a graph in Microsoft Excel, and then interpolation was used to determine the protein concentrations of the SE 16 and the SE 15 lab stock protein.

4.4g Redo of SE 15 Expression, Purification, Dialysis, and Protein Concentration

The large scale expression that was performed again for SE 15 was carried out very similarly to the above mentioned procedure. The purification process was also the same except that there were fewer Ni-NTA beads added with the ratio being one milliliter of beads to nine milliliters of supernatant. Additionally, dialysis was only done for three days. The protein concentration of SE 15 was calculated using a BCA.

4.4h Circular Dichroism

For circular dichroism the concentration of the SE 16 and an SE 15 lab stock protein were both around 0.20 milligrams/milliliter. The samples had a volume of 400 microliters. An AVIV CD Spectrometer Model 410 (Biomedical Inc.) instrument was used. The software used to run the instrument was the AVIV 410 CD. The wavelength of light used was from 190 nanometers to 260 nanometers. The temperature was set for twenty five degrees Celsius, and the bandwidth was one nanometer. The samples were exposed to each wavelength for four seconds. The results were graphed as an average of three values in Microsoft Excel and were deconvoluted using the website DichroWeb. Specifically the algorithm used was Contin-LL and the reference set was number seven.

4.4i UV-Vis Spectroscopy

First the SE 15 lab stock sample and the SE 16 sample had to be concentrated using fifty milliliter conical tubes with cassettes in them (Falcon). About eleven milliliters of each of the proteins were concentrated. The concentrations were then determined using BCA Protein Assay and were 1.5 milligrams/milliliter for SE 15 and 1.2 milligrams/milliliter for SE 16. 400 microliters of each sample were used for the experiment. An AVIV Spectrophotometer Model M (Biomedical Inc.) was the spectrophotometer used in the experiment. The software used was AVIV Model 14 Spectro. The samples were exposed to a wavelength of 300 nanometers and a bandwidth of one nanometer. The temperature rose in steps of five degrees from twenty degrees Celsius to 100 degrees Celsius and the back down to twenty degrees Celsius. Data was plotted in Microsoft Excel and was analyzed using information from previous research done in silk-elastinlike proteins (Nagarsekar 2002).

4.4j Fourier Transform Infrared Spectroscopy

A lab stock of SE 16 protein along with SE 15 protein were concentrated to five milligrams per milliliter and were used to make films in preparation for FTIR. 200 microliters of each protein solution was deposited on circular PDMS substrates ten centimeters in diameter. One film was made for each protein. The films were pretreated in about one milliliter of methanol for two hours and then dried for two hours. FTIR measurements were made both before and after the films were treated with methanol. A Fourier Transform/ Infrared Spectrometer 6200 (JASCO) was used in this experiment along with the computer program Spectra Manager. The range for the experiment was from 4000-600 cm^{-1} and the resolution was 4 cm^{-1}. A background spectrum was measured for each film and was subtracted from the experimental spectrums. Data was analyzed using Microsoft Excel.

4.4k Atomic Force Microscopy

SE 15 and a lab stock of SE 16 both at concentrations of one milligram/milliliter were used to make films on silicon wafers measuring four millimeters by five millimeters. The amount of protein deposited in each case was twenty microliters. A Dimension 3100 Atomic Force Microscope (Veeco) along with the software program Research Nanoscope 7.30 were used in the experiment. A Class 2M Laser was used with a one milliwatt maximum at 670 nanometers. The experimental tip (Veeco) had a spring constant between one and five Newtons per meter. Tapping mode was used for all imaging while force extension curves were done in contact mode. One film for each sample was examined. Data was analyzed using Research Nanoscope 7.30 as well as a manual detailing the analysis of AFM spectroscopy (Owen).

4.5 Results

4.5a Small Scale Expression

The results from small scale expression display all of the proteins detected in the SE 15 and SE 16 samples at time periods of zero hours, two hours, and four hours after induction with IPTG in the form of an SDS-PAGE gel (Figure 4). The molecular weights ranged from 10-160 kilodaltons. Specifically, the bands at a molecular weight of 60 kilodaltons in both SE 15 and SE16 appear to get darker as the time after induction increases. The bands at molecular weights of 40 and 50 kilodaltons do not get lighter or darker after induction.

Figure 4. An SDS-PAGE readout from small scale expression of SE 15 and SE 16. Briefly, glycerol stocks were cultured in LB medium containing kanamycin and induced to overexpress SE 15 or SE16 with IPTG. Samples were taken after 0, 2, and 4 hours. They were then loaded onto a Novex 4-12% Bis-Tris Gel with 1 X MES Running Buffer. The gel was stained using a Colloidal Blue staining kit (Invitrogen) and imaged using a gel box blank with a software.

4.5b Large Scale Expression

The results from SDS-PAGE of purified SE 15 and SE16 samples in the elution B, C, D, and E buffers are shown in Figure 5. In both SE 15 and SE 16 there are a few traces of proteins detected in the Buffer B samples. However, in buffers C, D, and E there are many different proteins detected. The bands at 60 kilodaltons, corresponding to that of silk-elastinlike protein are found in buffers C, D, and E in both SE 15 and Se 16 samples. Their presence in SE 15 is highest in buffer E. Also, the SE 15 buffer samples display a protein of a molecular weight just above 60 kilodaltons. In SE 16 samples, the silk-elasinlike protein is found almost exclusively in buffer E and is a very dark solid band. The yield of SE 16 was 30 mL of protein solution at a concentration of 0.318 mg/mL with a pH of 4.5.

Figure 5. An SDS-PAGE readout from purified SE 15 and SE 16 samples in elutions buffers B, C, D, E. Briefly large scale expression was carried out using glycerol stocks of BL 21 bacteria containing the gene for production of SE 15 and SE 16 were cultured in LB medium containing kanamycin. The cells were centrifuged and the supernatant was discarded. They were then lysed using a lysing buffer containing urea and Ni-NTA beads were added. The Ni-NTA bead solution was then passed through columns. Buffers B, C, D, and E were then added to the columns and flow through was collected to be used in samples for SDS-PAGE.

4.5c Redo of SE 15 Expression and Purification

The results from the SDS-PAGE reexpressed and repurified SE 15 samples in elution buffers B,C, D, and E are show in Figure 6. The column directly to the left of the samples with elution buffer B represents the flow through from when the Ni-NTA beads were added to the buffer B solution after cellular debris had been discarded. A protein at a molecular weight of 60 kilodaltons is detected strongly in Buffer C and D as well as a little less in Buffer E. Other

cellular proteins are only detected faintly Buffer C and not in Buffer D or E. The yield for SE 15 was about 100 mL of protein at a concentration of 5.2 mg/mL and a pH of 5.9.

Figure 6. An SDS-PAGE readout from repurified SE 15 samples in elutions buffers B, C, D, E. Briefly large scale expression was carried out using glycerol stocks of BL 21 bacteria containing the gene for production of SE 15 were cultured in LB medium containing kanamycin. The cells were centrifuged and the supernatant was discarded. They were then lysed using a lysing buffer containing urea and Ni-NTA beads were added. The Ni-NTA bead solution was then passed through columns. Buffers B, C, D, and E were then added to the columns and flow through was collected to be used in samples for SDS-PAGE.

4.5d Circular Dichroism

The results for circular dichroism measurements after deconvolution of SE 15 and SE 16 samples are seen in Figure 7. The deflection of right circular polarized light as indicated by mean residue ellipticity values is virtually the same for both SE 15 and SE16. The maximum values for both SE 15 and SE 16 are just below 500 degrees cm^2 $dmol^{-1}$ $residue^{-1}$ at wavelength values near 203 nm and 230 nm. The minimum value for both samples is around 2000 degrees cm^2 $dmol^{-1}$ $residue^{-1}$ at a wavelength of about 198 nm. The range of deflection is also roughly the same for both SE 15 and SE 16.

Figure 7. CD results for SE 15 and SE 16 after deconvolution. The sample volume used was 400 microliters and the concentration of each protein was 0.20 milligrams per milliliter. An AVIV CD Spectrometer Model 410 (Biomedical Inc) along with AVIV software were used. The wavelength of ultraviolet used was from 190 to 260 nanometers and samples were exposed to each wavelength for four seconds. The temperature was set to twenty five degrees Celsius. A plot of the circular dichroism measured in millidegrees versus wavelength was made using Microsoft Excel before being deconvoluted using the website DichroWeb.

The secondary structure of both SE 15 and SE 16 was quantified as seen in Figure 8. The algorithm used by the program Contin-LL produced the two best matches for each sample. All four resulting secondary structures have very similar amounts of alpha helices, beta sheets, turns, and unordered structures. From the diagram it can be see that the secondary structures of both proteins are mainly composed of unordered structures, beta sheets, and turns. Alpha helices are present in only a small amount in each sample.

Figure 8. Secondary structure quantification for SE 15 and SE 16. Deconvolution was performed using the website DichroWeb and specifically the program Contin-LL. The two sequences listed for each samples refer to the two best matches that the algorithm could find for the experimental sample. In the tables, helix refers to alpha helices while strands refer to beta sheet. Both SE 15 and SE 16 are mainly composed of unordered structures, beta sheets, and turns.

4.5e UV-Vis Spectroscopy

The results for UV-Vis Spectroscopy are seen for SE 15 in Figure 9. The absorbance of the SE 15 sample does not change as the temperature is increased from twenty degrees to one hundred degrees. Additionally, the absorbance does change as the temperature is cooled from one hundred degrees to just above sixty degrees. Therefore, no transition temperature could be calculated for SE 15.

Figure 9. A profile of the UV spectroscopy performed on an SE 15 sample. The concentration of the protein used was 1.5 milligrams per milliliters, and the volume of the sample was 400 microliters. An AVIV Spectrophotmeter Model M (Biomedical Inc) was used in the experiment as well as the AVIV Model 14 Spectro. The samples were exposed to a wavelength of 300 nanometers and a bandwidth of one nanometer. The temperature rose in steps of five degrees from twenty degrees Celsius to 100 degrees Celsius and the back down to twenty degrees Celsius. Data was plotted in Microsoft Excel.

The absorbance of the SE 16 sample can be seen in Figure 10. It stays constant as the sample is heated from twenty degrees Celsius until just above sixty degrees Celsius, but then it increases dramatically as the sample is heated to one hundred degrees Celsius. Next, when the sample was cooled from one hundred degrees Celsius the absorbance decreases sharply until it reaches its original level around sixty degrees Celsius. The transition temperature for SE 16 was found to be around 70^{o} Celsius.

Figure 10. A profile of the UV spectroscopy performed on an SE 16 sample. The concentration of the protein used was 1.5 milligrams per milliliters, and the volume of the sample was 400 microliters. An AVIV Spectrophotmeter Model M (Biomedical Inc) was used in the experiment as well as the AVIV Model 14 Spectro. The sample was exposed to a wavelength of 300 nanometers and a bandwidth of one nanometer. The temperature rose in steps of five degrees from twenty degrees Celsius to 100 degrees Celsius and the back down to twenty degrees Celsius. Data was plotted in Microsoft Excel.

4.5f Fourier Transform Infrared Spectroscopy

The FTIR results for SE 15 are displayed in Figure 11. It should be noted that the methanol treated film has a lower absorbance than the untreated film. In addition, the absorbance peak is seen at 2000 cm^{-1} for the untreated film. The minimum absorbance is -0.2 while the peak absorbance is about 0.4 both of which are for the untreated film. The FTIR results for SE 16 are displayed in Figure 12. The untreated film has a higher absorbance than the methanol treated film until slightly before 2000 inverse centimeters. Then the methanol film has a higher absorbance from that point until just before 3000 inverse centimeters. At the juncture the films have similar absorbances. The maximum absorbance, which was for the methanol treated film is nearly 0.6, while the minimum absorbance, which was for the untreated film is just over -0.4. For both the SE 15 and SE 16 films there is a high amount of noise and therefore no deconvolution was performed.

Figure 11. A profile of FTIR analysis performed on SE 15. 200 microliters of the protein solution was deposited on circular PDMS substrates ten centimeters in diameter. The films were pretreated about one milliliter of methanol for two hours and then dried for two hours. FTIR measurements were made both before and after the films were treated with methanol. A Fourier Transform/ Infrared Spectrometer 6200 (JASCO) was used in this experiment along with the computer program Spectra Manager. A background spectrum was measured for each film and was subtracted from the experimental spectrums. The range for the experiment was from 4000-600 cm^{-1} and the resolution was 4 cm^{-1}. Data was analyzed using Microsoft Excel.

Figure 12. A profile of FTIR analysis performed on SE 16. 200 microliters of the protein solution was deposited on circular PDMS substrates ten centimeters in diameter. The films were pretreated about one milliliter of methanol for two hours and then dried for two hours. FTIR measurements were made both before and after the films were treated with methanol. A Fourier Transform/ Infrared Spectrometer 6200 (JASCO) was used in this experiment along with the computer program Spectra Manager. A background spectrum was measured for each film and was subtracted from the experimental spectrums. The range for the experiment was from 4000-600 cm^{-1} and the resolution was 4 cm^{-1}. Data was analyzed using Microsoft Excel.

4.5g Atomic Force Microscopy

Images of aggregated particles for SE 15 and SE 16 proteins are displayed in Figure 13. In both images the particles appear to be circularly shaped. The size of the particles for both proteins vary. The force curves for SE 15 and SE 16 are shown in Figure 14. The y axis refers to

the deflection of the cantilever while the x axis refers to the depth at which the tip is sampling the surface. The darker blue curve on each graph displays the cantilever tip approaching and making contact with the protein films. The light blue curve on each graph displays cantilever tip retracting from the protein film. The deflection error for the SE 16 protein film seems to be more negative than that of the SE 15 film. Also, the retraction and approach curves for SE 15 are not linear at heights directly above the sample, while they are for SE 16. Additionally, the difference between the areas of the approach and retract curves is greater in SE 16 than in SE 15. Thus the resilience of SE 16 is greater than the resilience of SE 15.

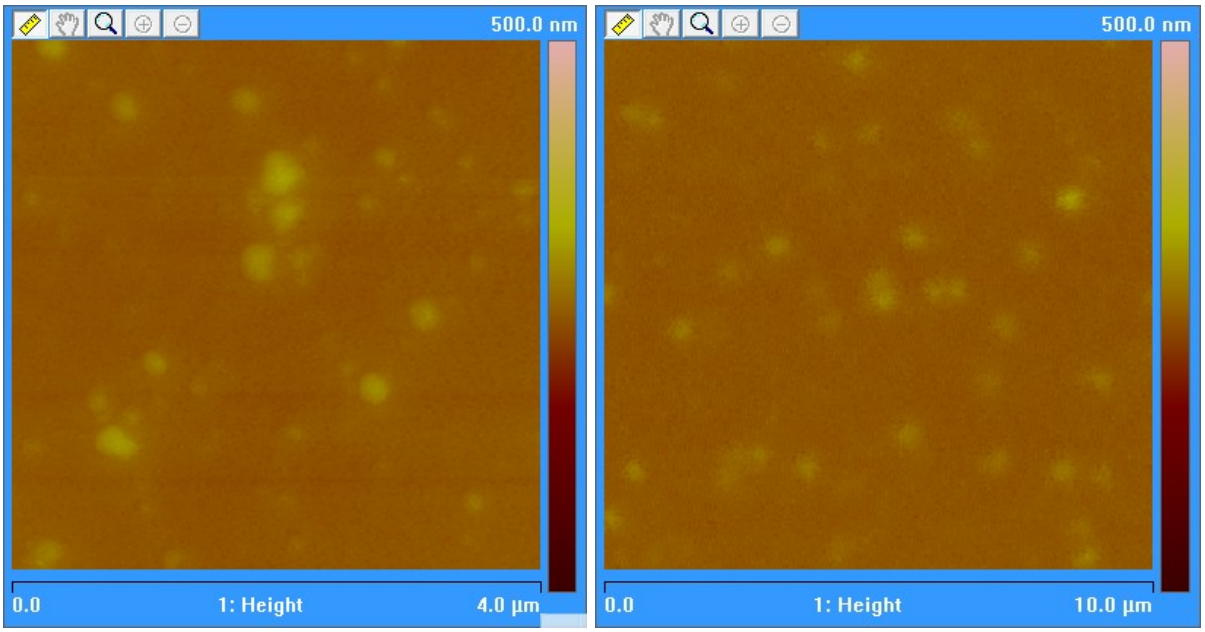

Figure 13. AFM images of SE 15 (left) and SE 16 (right). SE 15 and a lab stock of SE 16 both at concentrations of one milligram/milliliter were used to make films on silicon wafers measuring four millimeters by five millimeters. The amount of protein deposited in each case was twenty microliters. A Dimension 3100 Atomic Force Microscope (Veeco) along with the software program Research Nanoscope 7.30 were used in the experiment. A Class 2M Laser was used with a one milliwatt maximum at 670 nanometers. The experimental tip (Veeco) had a spring constant between one and five Newtons per meter. Tapping mode was used for all imaging.

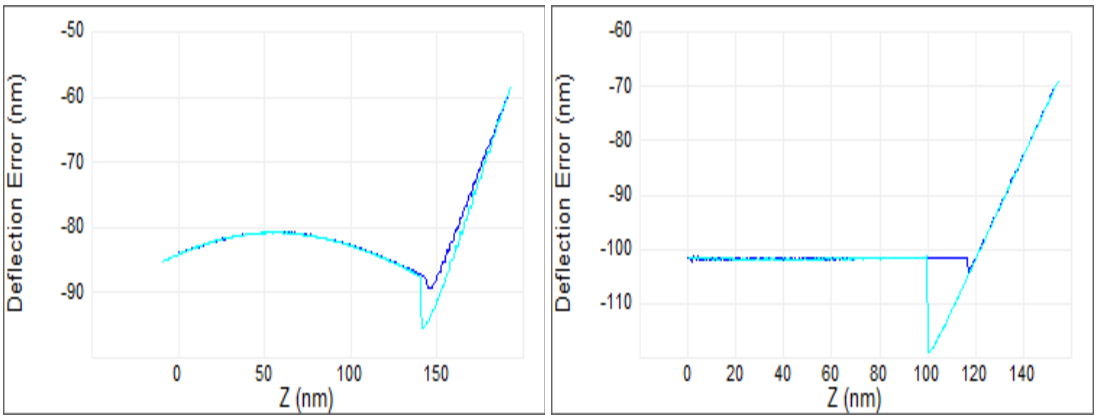

Figure 14. Force curves for SE 15 (left) and SE 16 (right). The darker blue curve represents the tip approaching the surface of the protein film while the lighter blue color represents the tip retracting off the surface of the film. SE 15 and a lab stock of SE 16 both at concentrations of one milligram/milliliter were used to make films on silicon wafers measuring four millimeters by five millimeters. The amount of protein deposited in each case was twenty microliters. A Dimension 3100 Atomic Force Microscope (Veeco) along with the software program Research Nanoscope 7.30 were used in the experiment. A Class 2M Laser was used with a one milliwatt maximum at 670 nanometers. The experimental tip (Veeco) had a spring constant between one and five Newtons per meter. Contact mode was used for all force extension curves. One film for each sample was examined. Data was analyzed using Research Nanoscope 7.30 as well as a manual detailing the analysis of AFM spectroscopy (Owen).

5. Discussion

The optimal conditions for expression of SE 15 and SE 16 were determined by overexpressing the gene for the proteins in bacteria and then by purifying the protein produced by the cells. The results of the small scale expression display an SDS PAGE gel showing all of the proteins at various molecular weights produced in cultured BL-21 cells after induction with IPTG in both SE 15 and SE 16 are seen in Figure 4. The particular band of interest is the protein found at a molecular weight of 60 kilodaltons. The bands on this protein appear to become darker and darker as the time after induction of IPTG increases. This is not the case as for other proteins as the bands at other molecular weights appear the same shade of darkness. Thus, it was determined that this band and molecular weight corresponded to the silk-elastinlike protein expression. Inducing the overexpression with IPTG was successful as more of the protein was produced as the molecules of IPTG continued to interact with lac operon in the plasmid encoding for the production of the protein.

Large scale expression and purification of SE 15 and SE 16 was seen in Figure 5. It appears as though that SE 15 was produced as evidenced by the dark bands found in Buffers C, D, and E at a 60 kilodaltons. However, the yield on the protein is undesirable and this may occurred for a few reason. First of all there may have been contamination with other cellular proteins bonding non specifically to the Ni-NTA beads. Additionally, there may have been an elevated level of proteases in the cell that degraded SE 15 proteins. The production of SE 16 was also seen in particular in Buffer E. This band in particular appears to be a well purified form of this silk-elastinlike protein. The yield of this protein was found to be 30 mL of protein solution at a concentration of 0.318 mg/mL. The pH of the elution buffer that produced this buffer is 4.5. This pH can be compared to that of the elution buffer for SE 15 show in Figure 6. First of all, the lack of other cellular proteins demonstrates that non specific protein binding to the beads was the results of a lack of pure SE 15 protein produced in the first instance. This is the case as fewer beads were used for the repurification of the silk-elastinlike protein. In addition, the best elution buffer for SE 15 was found to be Buffer D, which has a slightly higher pH of 5.9. The yield of SE 15 was greater in volume at 100 mL and in concentration at 5.2 mg/mL than SE 16. The difference in the pH levels for the optimal production of SE-15 and SE-16 can in part be explained by the difference in the purification process, which was using fewer metallic beads in column chromatography of SE 15. The use of fewer beads allowed for the binding of proteins to the beads to be more specific. This lead to a more optimized purficiation and ultimately production process for SE 15 than SE 16. Thus, the yield and concentration for SE 15 were greater than the yield for SE 16. The differences in pH values can be attributed to the greater yield of SE 15 produced. Since production was so much better optimized for SE 15, the protein

did not wait to elute in the typical elution buffer E with pH 4.5. Instead, a large amount of SE 15 protein eluted at a pH of 5.9 in buffer D as there was simply a higher yield.

The secondary structures of both of the proteins were examined using circular dichroism and FTIR (Figures 7, 8, 11, 12). The results of the circular dichroism demonstrate that the secondary structures of both proteins are extraordinarily similar. They show that the proteins are somewhere between 41 and 43 percent unordered structures, 18 percent turns, between 33 and 36 percent beta sheets, and a small amount (5 percent or less) of alpha helices. These results do coincide well with the fact that both silk and elastin are mostly composed of beta sheets, turns, and unordered structures. Thus, the secondary structure of silk-elastinlike proteins does not differ much from the secondary structure of both its silk and elastin components. Also, the numbers of silk and elastin units in the protein do not seem to affect its secondary structure. The results of the FTIR experiments can neither confirm nor deny those of circular dichroism. This is the case as subtracting out the background reveals that there is no difference in absorbance for films treated with methanol. This should not be the case as methanol treated films should increase the secondary structure interactions of proteins causing them to be illuminated more by the infrared light. Additionally, deconvolution was not performed on the FTIR results due to the large amount of noise in the results. While this is a necessary step in order to quantify secondary structure, in this instance the results of deconvolution would have proven to be inconclusive due to the large amounts of noise. The phenomenon of increased protein interactions after treatment with methanol was observed when trying to place the films on the stage for FTIR as they were curving and would not lie flat. The fact that the methanol films could not lie flat hampered them from making direct contact with the crystal. This may have contributed to the large amount of noise seen in the FTIR results. Furthermore, the untreated films should have also displayed

some sort of peaks indicating secondary structure formation but this was also not seen. Thus, the preparation of films using PDMS molds resulted in films that were too thin.

The transition temperature of both silk-elastinlike proteins was investigated using UV-Vis Spectroscopy as seen in Figure 9 and Figure 10. The results of this experiment indicate that SE 15 does not display transition temperature behavior while SE 16 does. In fact, the transition temperature of SE 16 can be approximated using the average of the highest and lowest absorbance values to be around seventy degrees Celsius. The disparity between SE 15 and SE 16 can be attributed to the fact that SE 15 contains more silk residues and fewer elastin residues than SE 16. It is elastin, not silk that exhibits a unique transition temperature behavior. Thus, when the temperature is raised above this point, a protein solution with SE 16 will have increased absorbance as more of the protein falls out of solution and aggregates together.

Finally, the resilience of both SE 15 and SE 16 proteins was examined using AFM. The images of the silk-elastinlike particles in SE 15 and SE 16 in Figure 13 reveal the circular shape of protein particles found in the solution. These protein molecules seem to clump together explaining the larger and smaller circular objects observed in the images. The force curves in Figure 14 do demonstrate the resilience of both proteins. This resilience can be estimated by observing the ratio of the area of the approach curve to that of the retract curve (Hu 2010). There is a greater disparity between these two curves in SE 16 as there is in SE 15. This can be interpreted as the resilience in SE 16 being less than that of SE 15. This makes sense as SE 15 contains more silk units than SE 16. Silk exhibits its properties of resilience and strength in silk-elastinlike proteins as well.

While the most of the aims of this experiment were accomplished, there are many different changes that could have been made to this experiment to improve the quality of results

of future experiments. This is with particularly regards to the material characterization tests but not limited to it. More SE 15 and SE 16 needed to be produced as some lab stock had to be used for materials testing. This could have been easily accomplished by inoculating more of the glycerol stocks for small and then large scale expression. In addition, more replicates for each of the materials testing should have been performed to allow for statistical significance and standard error calculations. Furthermore, the purity of the SE 15 and SE 16 protein should have been quantified as well as the amount. The purity could have been quantified to ensure better results for materials testing particularly CD and FTIR. This could have been done by using different dilutions of the SE 15 and SE 16 samples on an SDS PAGE gel. Additionally, mass spectroscopy could have been used to quantify the amount of protein produced in the cells, which could lead to further optimization production experiments. Also, the films made for FTIR were ineffective and a different process other than using PDMS molds needs to be used. When they are treated with methanol, the films stuck together and for future experiments need to be held flat when they are being dried. Furthermore, there needed to be more analysis done on the FTIR results specifically deconvolution. Lastly, there needs to be more analysis done on the images and force extension curves for AFM to determine material properties such as the elastic modulus. In fact, if large enough films on the order of centimeters could be created for possible use in FTIR and AFM, then there use could be expanded to test for other properties such as tensile strength.

6. Conclusion

In conclusion, the optimal pH levels of SE 15 and SE 16 were able to be assessed. The yield of SE 15 was found to be 100 mL of protein solution with a concentration 5.2 mg/mL with a pH of 5.9. The yield of SE 16 was found to be 30 mL of protein solution with a concentration

of 0.318 mg/mL and a pH of 4.5. The difference in the yields of the protein as far as amount and concentration were determined to be due to the number of metallic beads using the in Ni-NTA column chromatography purification process. In regard to the difference in pH, this was found to be directly correlated to the differences in yield. Thus, it can be concluded that the range of pH values for the protein solution for silk-elastinlike proteins is directly dependent on the yield of the proteins. The two proteins were also able to be expressed and purified using genetic engineering and column chromatography. SE 16 was found to exhibit transition temperature behavior with a transition temperature of 70^{o} Celsius while SE 15 did not using UV-Vis Spectroscopy. Additionally, deconvolution of circular dichroism results demonstrated that the two proteins have similar secondary structures containing around 41 to 43 percent unordered structures, 33-36 percent beta sheets, 18 percent turns, and a small amount of alpha helices. The large amount of unordered structures and beta sheets corresponds with the secondary structures of silk and elastin. The similarity of the secondary structures was a result of the two silk-elastinlike proteins being composed of the same two proteins, silk and elastin. FTIR results could not confirm this assessment as no deconvolution was performed due to noisy results. Finally, AFM was used to image the nanostructures of the proteins while suggesting that SE 15 was more resilient than SE 16 using force curves. Overall, the number of silk units and elastin units found in the silk-elastinlike proteins was found to impact the transition temperature and resilience of the two proteins but not the secondary structure. In particular, SE 16 was shown to exhibit transition temperature behavior and was more resilient that SE 15, which did not show transition temperature behavior. However, the number of silk and elastin units did not seem to affect secondary structure of the two silk-elastinlike proteins.

7. Future Work

There are many future directions that can be taken based off the results of this experiment. The short term future directions would involve replicating the experiments in this study and making the aforementioned changes in particular with regards to the film construction. Additionally, further materials testing could be carried out investigating such properties as elasticity, Young's modulus, and tensile strength. Once the structural and material properties of the silk-elastinlike proteins are well document, the production of these proteins can be optimized to achieve the desired material properties. At this juncture specific silk-elastinlike proteins could then have their production optimized to be constructed as different components of a soft bodied robot.

The long term future direction of this study is the creation of a biocompatible, biodegradable soft bodied robot. One of these potential uses could be as a material for a Chembot to satisfy the requirements of a U.S. Defense Advanced Research Projects Agency (DARPA). This project for which a $3.3 million dollar grant was given to Tufts University in 2008, is intended to create a robot that is soft and squishy (Tufts to Develop Morphing Robots 2010). This robot will be able to squeeze into a space as small as one centimeter and then expand into something ten times larger. Some of the tasks the robot will need to accomplish include the ability to fit through small, complex spaces, climb branched structures, and follow cables or wires (Trimmer 2006).

Tufts University was able to achieve the money for this grant largely through work a soft body caterpillar robot led by Barry Trimmer (Tufts to Develop Morphing Robots 2010). The current prototype of this caterpillar robot built by Tufts University is composed of a commercial soft silicone elastomer that is more commonly known as Dragonskin (Trimmer 2006). Dragonskin is able to stretch to many times its original volume and can go back to its original

form with little to no distortion (Dragon Skin High Performance Silicone Rubber 2010). It is very strong and can be used in such applications as casting concrete and wax. This material is not very biocompatible or biodegradable. Therefore, in order to use soft bodied robots in medicine it would be best to use a biocompatible, biodegradable material such as a silk-elastinlike protein. Ultimately, the results and conclusions of this experiment determined that much more research is needed before silk-elastinlike proteins can be used in the construction of soft bodied robots.

8. References

Altman, Gregory H., Frank Diaz, Caroline Jakuba, Tara Calabro, Rebecca L. Horan, Jingsong Chen, Helen Lu, John Richmond, and David L. Kaplan. "Silk-based Biomaterials." *Biomaterials* 24.3 (2003): 401-16. *Science Direct*. Web. 4 May 2010.

Dandu, Ramesh, Arthur Von Cresce, Robert Briber, Paul Dowell, and Joseph Cappello. "Silk–elastinlike protein next term polymer hydrogels: Influence of monomer sequence on physicochemical properties ." *Polymer* 50.2 (2008): 366-374. Web. 14 Apr 2011.

Debelle, Laurent, and Alain Alix. "The Structures of Elastins and their Function." *Biochimie* 81.10 (1999): 981-994. Web. 9 May 2011.

Dutoya, S., A. Verna, F. Lefebvre, and M. Rabaud. "Elastin-derived Protein Coating onto Poly(ethylene terephthalate). Technical, Microstructural and Biological Studies ." *Biomaterials* 21.15 (2000): 1521-1529. Web. 9 May 2011.

Dinerman, Adam, Joseph Cappello, Hamidreza Ghandehari, and Stephen Hoag. "Solute diffusion in genetically engineered silk–elastinlike protein polymer hydrogels." *Journal of Controlled Release* 82.2-3 (2002): 277-287. Web. 14 Apr 2011.

"Dragon Skin® High Performance Silicone Rubber | Smooth-On, Inc." *Smooth-On - Mold Making and Casting Materials for a World of Applications!* Web. 04 May 2010. <http://www.smooth-on.com/Silicone-Rubber-an/c2_1115_1129/index.html>.

Gallagher, William. "FTIR Analysis of Protein Structure." *Chem 455- Spring 2005*. University of Wisconsin-Eau Claire, 2005. Web. 10 May 2011.

Greenfield, Norma. "Using Circular Dichroism to Estimate Protein Secondary Structure." *Nature* 1.6 (2006): 2876-2890. Web. 9 May 2011.

Gustafson, Joshua, and Hamidreza Ghandehari. "Silk-elastinlike protein next term polymers for matrix-mediated cancer gene therapy." *Advanced Drug Delivery Reviews* 62.15 (2010): 1509-1523. Web. 14 Apr 2011.

Hu, Xiao, Xiuli Wang, Jelena Rnjak, Anthony Weiss, and David Kaplan. " Biomaterials derived from silk–tropoelastin protein systems ." *Biomaterials* 31.32 (2010): 8121-8131. Web. 14 Apr 2011.

Lee, Jonghwi, Christopher W. Macosko, and Dan W. Urry. "Elastomeric Polypentapeptides Cross-Linked into Matrixes and Fibers." *Biomacromolecules* 170.2 (2001): 170-79. Web. 4 May 2010.

McClements, Julian. "Analysis of Proteins." *Analysis of Food Products*. University of Massachusetts, n.d. Web. 10 May 2011.

Megeed, Zaki, Joseph Cappello, and Hamidreza Ghandehari. " Genetically engineered silk-elastinlike next term protein polymers for controlled drug delivery ." *Advanced Drug Delivery Reviews* 54.8 (2002): 1075-1091. Web. 14 Apr 2011.

"Introduction to Fourier Transform Infrared Spectroscopy." *Molecular Materials Research Center*. Thermo Nicolet Corporation, 2001. Web. 10 May 2011.

Nagarsekar, Ashish, John Crissman, Mary Crissman, Franco Ferrari, and Joseph Cappello. "Genetic Synthesis and Characterization of PH- and Temperature Sensitive Silk-elastinlike Protein Block Copolymers." *Journal of Biomedical Research* 62.2 (2002): 195-203. *Wiley Periodicals*. Web. 4 May 2010.

Ner, Yogesh, Jeffrey A. Stuart, Gregg Whited, and Gregoy A. Sotzing. "Electrospinning Nanoribbons of a Bioengineered Silk-elastin-like Protein (SELP) from Water." *Polymer* 50.24 (2009): 5828-836. *Science Direct*. Web. 4 May 2010.

Nuhn, Harald, and Harm-Anton Klok. "Secondary Structure Formation and LCST Behavior of Short Elastin-Like Peptides." *Biomacromolecules* 9.10 (2008): 2755-763. *American Chemical Society*. Web. 4 May 2010.

Owen, Rachel. *A Practical Guide to AFM Spectroscopy and Data Analysis*. Tech. JPK Instruments. Web. 4 May 2010.

Prince, John T., Kevin P. McGrath, Carla M. DiGirolamo, and David L. Kaplan."Construction, Cloning, and Expression of Synthetic Genes Encoding Spider Dragline Silk." *Biochemistry*. 34. (1994): 10879-10885. Print.

Sallach, Rory, Wanxing Cui, Jing Wen, Adam Martinez, and Vincent Conticello. "Elastin-Mimetic Protein Polymers Capable of Physical and Chemical Crosslinking." *Biomaterials* 30.3 (2009): 409-422. Web. 9 May 2011.

Trimmer, Barry A., Ann E. Takesian, Brian M. Sweet, Chris B. Rogers, Dan C. Hake, and Daniel J. Rogers. "Caterpillar Locomotion: A New Model for Soft Bodied Climbing and Burrowing Robots." (2006). 7th International Symposium on Technology and the Mine Problem. Web.

"Tufts to Develop Morphing Chemical Robots." *Tufts E-News: Daily News. Tufts University's Official Electronic News Source.* Web. 04 May 2010. <http://enews.tufts.edu/stories/168/2008/06/30/TuftstoDevelopMorphingChemicalRobots>.

Urry, Dan W., and Asima Pattanaik. "Elastic Protein-based Materials in Tissue Reconstruction." *Bioartificial Organs: Science, Medicine, and Technology* 831 (1997): 32-46. *Wiley Interscience*. Web. 4 May 2010.

Valiaev, Alexei, Dong Woo Lim, Scott Schmidler, Robert L. Clark, Ashutosh Chilkoti, and Stefan Zauscher. "Hydration and Conformational Mechanics of Single, End-Tethered Elastin-like Polypeptides." *American Chemical Society* (2008). Web.

Vepari, Charu, and David L. Kaplan. "Silk as a Biomaterial." *Progress in Polymer Science* 32.8-9 (2007): 991-1007. *Science Direct*. Web. 4 May 2010.